Integrator-mediated clustering of poised RNA polymerase II synchronizes histone transcription

Feiyue Lu[1], Brandon J. Park[2,†], Rina Fujiwara[3], Jeremy E. Wilusz[3], David S. Gilmour[2], Ruth Lehmann[4,5] and Timothée Lionnet[1,6,7]*

[1]Institute for Systems Genetics, NYU Grossman School of Medicine, New York, NY 10016, USA.
[2]Center for Eukaryotic Gene Regulation, Department of Biochemistry and Molecular Biology, The Pennsylvania State University, University Park, PA 16802, USA.
[3]Verna and Marrs McLean Department of Biochemistry and Molecular Pharmacology, Therapeutic Innovation Center, Baylor College of Medicine, Houston, TX 77030, USA
[4]Whitehead Institute for Biomedical Research, Cambridge, MA 02142, USA.
[5]Department of Biology, Massachusetts Institute of Technology, Cambridge, MA 02139, USA.
[6]Department of Cell Biology, NYU Grossman School of Medicine, New York, NY 10016, USA.
[7]Department of Biomedical Engineering, NYU Tandon School of Engineering, Brooklyn, NY 11201, USA.
[†]Present address: Department of Biomedical Genetics and Genomics, University of Rochester, NY 14642, USA.
*Corresponding author. Email: timothee.lionnet@nyulangone.org

Abstract:
Numerous components of the transcription machinery, including RNA polymerase II (Pol II), accumulate in regions of high local concentration known as clusters, which are thought to facilitate transcription. Using the histone locus of *Drosophila* nurse cells as a model, we find that Pol II forms long-lived, transcriptionally poised clusters distinct from liquid droplets, which contain unbound and paused Pol II. Depletion of the Integrator complex endonuclease module, but not its phosphatase module or Pol II pausing factors disperses these Pol II clusters. Consequently, histone transcription fails to reach peak levels during S-phase and aberrantly continues throughout the cell cycle. We propose that Pol II clustering is a regulatory step occurring near promoters that limits rapid gene activation to defined times.

One Sentence Summary: Using the *Drosophila* histone locus as a model, we show that clustered RNA polymerase II is poised for synchronous activation.

Introduction:

Numerous regulators of eukaryotic transcription, including the major RNA-synthesizing enzyme, RNA polymerase II (Pol II (*1–9*)), co-activators (*3*, *7*, *10*), as well as general (*7*, *11*, *12*) and sequence-specific transcription factors (*13–15*), can assemble into membrane-less clusters. These clusters are mostly highly dynamic, short-lived, and exhibit liquid-like properties (*16*). Clustering of transcription regulators is dependent on the multivalent interactions of their

intrinsically disordered regions (IDRs) and is generally thought to be mediated by liquid-liquid phase separation (LLPS) (*3*, *4*, *10*, *11*, *17*, *18*), although LLPS-independent mechanisms could also be involved (*19–21*). Clustering has been thought to facilitate transcription by allowing for the rapid accumulation of high concentrations of regulatory molecules at the target genes (*22*), which is supported by recent observations that artificially induced clustering of transcription factors is sufficient to boost transcription (*23–25*).

Pol II clustering is mediated by the disordered C-terminal domain (CTD) of its largest Rpb1 subunit (*4*, *26–29*). Pol II is recruited to transcription sites largely unphosphorylated and is subsequently phosphorylated by CTD kinases at various stages of transcription (*28*, *30–32*). *In vitro*, the Pol II CTD alone can partition into hydrogels containing other transcription factor IDRs (*26*), is sufficient to form phase-separated clusters (*27*), and can incorporate into co-activator condensates (*4*), all of which are disrupted upon CTD phosphorylation. *In vivo*, Pol II forms numerous clusters that are liquid-like (*3*), CTD-length dependent (*27*), and correlate with transcription bursts (*2*, *5*). These findings led to the model that Pol II clustering occurs before transcription initiation whereas transcription-coupled phosphorylation of the CTD releases Pol II from clusters and allows for productive elongation (*26–28*). However, whether endogenous Pol II clustering constitutes a regulatory checkpoint in the cellular context remains untested. Here, we leveraged microscopy with genetic perturbations in the *Drosophila* ovarian nurse cells to investigate the dynamics, assembly, and activation of Pol II clustering at the histone locus and its regulatory roles in transcription.

Capturing Pol II clustering at the histone locus of the *Drosophila* nurse cells

Pol II clusters are often short-lived and range in size from diffraction-limited to sub-micron in diameter in most cells (*1–9*). Their detection thus typically requires either cutting-edge microscopic technologies with high spatiotemporal resolution or repetitive synthetic gene arrays that enable signal amplification. The histone locus in the *Drosophila* ovarian nurse cells (NCs) of developing egg chambers provide a unique, natural system for capturing Pol II clustering without the need for either of the aforementioned approaches. The NCs are endocycling cells with alternating G and S cycles that can amplify DNA to 1,000 n ploidy and reach 50 μm or more in nuclear diameter (*33*) (Fig. 1A). The most prominent Pol II clusters often reside on the replication-dependent histone genes (*6*, *8*, *9*, *34*), which in *Drosophila* are present in ~100 copies at a single locus (*35*). The histone locus self-organizes into membrane-less subnuclear compartments called histone locus bodies (HLBs) (*36*), which form one visible focus per NC in early egg chambers and multiple foci per NC in mid to late-stage egg chambers as DNA copy number increases (*37–39*) (Fig. 1B). The repetitiveness of the *Drosophila* histone locus combined with the polyploidy of NCs thus constitute a naturally occurring signal amplification platform for imaging Pol II clusters.

To visualize Pol II clustering, we generated a homozygous viable, Halo-tagged Pol II fly line by appending the tag to the C-terminus of the Rpb1 subunit following a previously described CRISPR/Cas9 editing scheme (*40*). Halo-tagged Rpb1 is expressed at endogenous levels, associates with chromosomes, and responds normally upon heat shock (fig. S1). In NCs from Stage 2 to 9 egg chambers, histone mRNAs are synthesized in S-phase and degrade upon exiting S-phase (*39*). Each egg chamber contains nurse cells engaged in different stages of the endocycle (*33*). Micron-sized HLB-bound Pol II clusters are observed in all S-phase NCs (N=109) when histone transcription is active. However, 72% of G-phase NCs (N=150) also contain visible HLB-bound Pol II clusters (Fig. 1B). Since each endocycle lasts for at least 7 hours in NCs (*33*), Pol II clusters must be present for substantial periods outside the window in which histone transcription takes place. To capture this phenomenon in live egg chambers, we used a fly line that expresses both Halo-Rpb1 and a cell cycle marker GFP-CycE (*33*), which localizes to S-phase HLBs (*36*, *39*) (fig. S2). Indeed, Pol II clusters form before entry into S-phase and persist hours after exiting S-phase (Fig. 1C, movie S1 and S2). The lack of Pol II clusters at HLBs over a fraction of G-phase is not simply due to the dispersion of HLBs: unlike in tissue-cultured cells or in the early fly embryos where HLBs gradually dissolve during cell division and reform upon mitotic exit (*8*, *36*, *41*), micron-sized HLBs (marked by HLB scaffolding protein Mxc) are present in all NCs regardless of cell cycle stages (*37–39*) (Fig. 1B), presumably due to the lack of cell division. This suggests that there must be separate mechanisms controlling Pol II clustering at HLBs from those regulating HLB assembly. Collectively, HLBs of NCs provide a highly tractable system that enables the observation of Pol II clustering with high spatiotemporal resolution at a native locus whose transcription activation is tightly coupled to the cell cycle.

The HLB-bound Pol II clusters do not show hallmarks of CTD-driven LLPS

If the formation of HLB-bound Pol II clusters is entirely driven by CTD-dependent LLPS, the following three predictions should be fulfilled. First, fluorescent Pol II molecules within clusters should exhibit diffusion-driven recovery upon bleaching. Contrary to this expectation, fluorescence recovery after photobleaching (FRAP) showed that HLB-bound Pol II does not recover fully, suggesting a substantial slow-exchanging subpopulation (recovered fraction ~0.63 to ~1.04; Fig. 2A to C). Furthermore, half-recovery times of HLB-bound Pol II (ranging from ~45 to 205s) are substantially slower than the seconds timescales observed previously for LLPS condensates (*3*, *4*, *27*) Both recovery parameters are similar to Pol II FRAP dynamics on polytene chromosomal loci (*42*). Second, treatment with 1,6-hexanediol (1,6-HD), a chemical sufficient for disrupting weak hydrophobic interactions, should dissolve Pol II clusters (*3*, *4*, *8*, *27*). However, the HLB-bound Pol II clusters survived treatment with 5% 1,6-HD, unlike P-bodies (marked by Me31B-GFP) that were largely dissolved (*43*) (Fig. 2D). Third, the propensity of Pol II clustering should increase as the CTD length increases (*27*). To directly compare the clustering propensity of Pol II molecules containing CTDs varying in length and sequence composition, we mated an endogenously HA-tagged wild-type Rpb1 (HA-Rpb1^{WT}) fly line to

various FLAG-tagged Rpb1 CTD variants (*44*) such that the resulting female progenies have a copy of each Pol II form. The stoichiometric ratios of the FLAG variants to HA-Rpb1^{WT} at HLBs do not increase with increasing CTD length, in opposition to the prediction of CTD-dependent LLPS model (Fig. 2E and fig. S3). While we cannot rule out the possibility that LLPS mediates some aspects of Pol II clustering, these observations argue that additional mechanisms must be involved in the formation of Pol II clusters.

Nearly all the HLB-bound Pol II molecules are transcriptionally inactive

The observation that Pol II clusters are present at HLBs in the majority of G-phase NCs suggests that a portion of the Pol II clusters are transcriptionally inactive. To confirm this, we measured Ser2 phosphorylation (Ser2ph) levels at HLBs. Ser2ph marks Pol II molecules that have advanced beyond the promoter-proximal regions of genes (*28*, *30*, *32*). Amongst all NCs analyzed, only 2.9% (N=448) showed visible levels of Ser2ph enrichment over nucleoplasm at HLBs (Fig. 3A), suggesting that high levels of histone transcription only take place during a tiny fraction of the clustering lifetime. To further validate this, we pulse-labeled egg chambers with 5-ethynyl uridine (EU) to detect nascent transcripts (*45*). Similar to Ser2ph, 3.0% of all NCs (N=311) contained HLB-bound Pol II clusters with detectable levels of EU incorporation (Fig. 3B, lower panels). The low Ser2ph and EU enrichment at HLBs is not due to insufficient sensitivity: besides HLBs, Pol II forms numerous sub-micron clusters in Stage 10 NCs, a fraction of which showed high Ser2ph (fig. S4 and movie S3) and EU enrichment (Fig. 3B, upper panels, blue arrows). Finally, to investigate whether transcription elongation is required for Pol II clustering at HLBs, we treated egg chambers with flavopiridol (FP), an inhibitor of the kinase P-TEFb which deposits the Ser2ph mark and releases paused Pol II into productive elongation (*46*). While FP effectively inhibits P-TEFb as indicated by reduced nuclear levels of Ser2ph (fig. S5) (*32*, *47*), Pol II clusters are not dissolved (Fig. 3C and D, movie S4). Together, these data argue that Pol II clustering occurs before pause release, with most Pol II molecules remaining inactive for a substantial period following recruitment to HLBs.

The HLB-bound clusters contain both promoter-proximal paused and unbound Pol II molecules

Since the vast majority of HLBs exhibit undetectable levels of productively transcribing Pol II, we next explored the possibility that the Pol II clusters contain promoter-proximal paused Pol II. We reasoned that if we depleted Spt6 or Spt5, two factors that sustain promoter-proximal pausing (*48*, *49*), paused Pol II should be released into the gene body. In consequence, if HLBs contained paused Pol II, their Ser2ph levels should increase upon Spt6 or Spt5 depletion. Indeed, upon RNAi depletion of Spt6 or Spt5, the levels of Ser2ph drastically increased at HLBs (Fig. 4A and B, fig. S6). This suggests that HLB-bound Pol II clusters are at least in part made up of promoter-proximal paused Pol II.

The observation of Pol II clusters highly enriched in Ser2ph upon depletion of pausing factors is seemingly at odds with models suggesting that CTD phosphorylation disrupts Pol II clusters coincidently with entry into productive elongation (*26–28*). This paradox could be reconciled if upon depletion of pausing factors, Pol II still pauses, but further downstream from the transcription start site. To test this possibility, we pulse-labeled egg chambers with EU and co-stained them for Ser2ph. In control, NCs with detectable levels of both EU uptake and Ser2ph enrichment were rarely observed (2.6%, N=270) and instead, almost all nuclei lacked both EU and Ser2ph signals at HLBs. Upon knockdown of Spt6 or Spt5, we found little EU incorporation at the HLB-bound Pol II clusters despite significant increases in the levels of Ser2ph (fig. S7). This suggests that the promoter-proximal escaped Pol II molecules are stalled further downstream on the template, consistent with recent observations with Spt5 (*49*).

Because our FRAP analyses revealed subpopulations of HLB-bound Pol II molecules with two distinct recovery kinetics regardless of cell cycle stages (Fig. 2A to C), we wondered whether other forms of Pol II besides paused Pol II might be present at HLBs – for instance unbound Pol II, defined here as Pol II molecules recruited to the vicinity of the promoter but not engaged in the pre-initiation complex or subsequent steps. As Pol II molecules transit from the unbound state to early initiation, their levels of Ser5 phosphorylation (Ser5ph) rapidly increase (*28, 30, 32*). We reasoned that treating egg chambers with the initiation inhibitor Triptolide (TRI) should only leave at the HLB stably paused Pol II (*50*), which has higher Ser5ph levels than unbound Pol II. If HLBs are solely constituted of Pol II molecules engaged at 5'-end of genes in unperturbed conditions, we should therefore observe little change in the Ser5ph:Pol II ratio at the HLB upon TRI treatment. The intensity of Pol II clusters at HLBs drastically decreased within 35 min of TRI treatment, consistent with loss of transcription initiation (Fig. 4C, movie S5 and fig. S8), and this decrease was not due to Pol II degradation (fig. S9). However, the ratios of Ser5ph:Pol II increased by nearly two-fold after normalizing by nuclear levels (Fig. 4D and fig. S8). This observation shows that in unperturbed conditions, Pol II clusters at HLBs exhibit a lower Ser5ph:Pol II ratio than that of paused Pol II, and therefore suggests that in addition to paused Pol II, they also contain a subpopulation of unbound Pol II.

The Integrator endonuclease module is required for Pol II clustering at HLBs

Since clusters at the histone locus contain promoter-proximal paused Pol II molecules, we examined whether depletion of the Integrator, a multi-subunit complex involved in promoter-proximal regulation of transcription, is sufficient to disrupt Pol II clustering. The Integrator complex consists of a phosphatase module and an endonuclease module (*51–54*). RNAi depletion of the Integrator endonuclease subunits IntS11 or IntS9 resulted in a complete loss of visible HLB-bound Pol II clusters in all NCs starting from Stage 6 (Fig. 5A and B, and fig. S10). In contrast to TRI treatment where the Ser5:Pol II ratio nearly doubled, the same ratio only

moderately increased upon IntS11 RNAi, suggesting that both promoter-proximal and unbound Pol II molecules were lost (Fig. 5C). Importantly, the loss of Pol II clusters upon IntS11 or IntS9 RNAi is not simply due to a global loss of HLB structure, as P-TEFb and the scaffolding protein Mxc remained present at HLBs (fig. S11). Nor is it due to RNAi-induced cell death, as IntS11 RNAi and IntS9 RNAi egg chambers did not show arrested development until Stages 10 and 9, respectively (fig. S12). RNAi depletion of IntS8, a key bridging subunit connecting the phosphatase module to the rest of the Integrator, (*55*, *56*) did not affect Pol II levels at HLBs (fig. S13). Collectively, these results establish the Integrator endonuclease module, but not its phosphatase module, as an essential regulator for Pol II clustering at HLBs.

Out-of-phase and reduced induction of histone transcription upon loss of the Integrator endonuclease

Since Integrator depletion leaves the HLB scaffold intact (Fig. 5 and fig. S11), it provides us with a tool to perturb Pol II clustering and study transcription outcomes independently of changes in the underlying HLB structure. If Pol II clustering simply enhanced transcription activity as previous models suggested, Integrator depletion should lead to a significant decrease in histone transcription. To visualize histone expression, we performed RNA fluorescence in situ hybridization (FISH) against H3 transcripts. In unperturbed conditions, S-phase NCs exhibit robust levels of H3 transcripts both at HLBs and in the cytoplasm, while G-phase NCs are essentially devoid of signal up to Stage 9, in agreement with a previous study in *Drosophila* NCs (Potter-Birriel et al. 2021) (Fig. 6A and fig. S14). Consistent with the low percentage of NCs showing Ser2ph staining at HLBs or EU uptake (Fig. 3A and B), 4.5% (9 out of 201) of all NCs express very high levels of H3 (z-score>2; Fig. 6B). RNAi depletion of IntS11 or IntS9 resulted in a narrower range of H3 expression, with a reduced higher quantile indicative of decreased levels of induction and an increased lower quantile compared to control (Fig. 6B and fig. S15B). The latter observation is inconsistent with models of clustering-facilitated transcription and could be attributed to either increased levels of H3 expression in G-phase NCs, increased percentages of S-phase NCs, or both. To eliminate any potential effects of cell cycle disruption, we restricted our analysis to G-phase NCs and confirmed that the majority of them expressed H3 upon IntS11 and IntS9 RNAi (Fig. 6C, fig. S15C and fig. S16). In contrast, RNAi depletion of Spt6 or Spt5 resulted in overall reduced expression but not aberrant expression in G-phase (fig. S17), suggesting that the leaky expression cannot be explained by the loss of promoter-proximal Pol II molecules.

The increased level of H3 mRNA in G-phase upon IntS11 and IntS9 RNAi can be triggered by either aberrant activation of histone transcription or disruption of histone mRNA degradation. We first examined the cytoplasmic mRNA levels of the ribosomal protein gene RpL30 and found that it does not display similar levels of increase upon either IntS11 or IntS9 RNAi (Fig. 6A and D and fig. S15A and D), arguing that IntS11 and IntS9 RNAi did not disrupt general mRNA

degradation pathways. Since histone transcripts are normally rapidly degraded upon exiting S-phase, and misprocessing of histone transcripts can lead to downstream degradation defects (*57*), we next investigated whether H3 mRNA is misprocessed upon IntS11 and IntS9 RNAi. In *Drosophila*, histone mRNA 3'-end processing consists of a cleavage step tightly coupled to transcription termination. Unprocessed histone transcripts can therefore be detected using mRNA FISH probes targeting regions downstream of the H3 pre-mRNA cleavage site (*36*, *39*) (Fig. 6E). In control NCs, the downstream H3 probe (DS-H3) detects unprocessed H3 transcripts at HLBs, consistent with observations in early embryos (*36*). H3 mRNA forms foci in the cytoplasm, which are marked by a probe against the H3 gene body (3'-H3), but not by the DS-H3 probe. The ratios of DS-H3 to 3'-H3 signals did not increase at HLBs nor in the cytoplasm upon IntS11 or IntS9 RNAi (Fig. 6F and G, fig. S15E and F), thus ruling out the effects of misprocessing on misexpression. Together, these results argue that the misexpression of H3 in G-phase upon depletion of the Integrator endonuclease is instead due to aberrant transcription activation.

Discussion

Clustering of the transcription machinery, particularly Pol II, has long been thought to boost transcription via mass-action (*58*). The clustering behavior of Pol II over the transcription cycle of the *Drosophila* histone locus challenges this model, since Pol II clustering takes place in the absence of active transcription. Indeed, loss of Pol II clustering via depletion of the Integrator endonuclease revealed opposing transcription outcomes at different cell cycle stages. In S-phase, loss of clustering reduces the level of transcription induction, consistent with the mass-action based model (*22–25*). In G-phase, however, loss of clustering leads to aberrant histone transcription, suggesting a repressive role in transcription and thus challenging the long-standing notion that transcription clusters simply enhance transcription activity. Furthermore, HLB-bound Pol II clusters do not show hallmarks of CTD-driven LLPS and persist in the presence of hyper-phosphorylation at either Ser2 or Ser5 residues of the CTD. This suggests that at least on the histone locus, Pol II clustering must be subjected to additional layers of regulation beyond CTD-phosphorylation-gated phase separation.

We propose that clustering might restrict the timing of histone transcription by sequestering poised Pol II molecules for rapid activation at designated times (Fig. 7). Several lines of evidence suggest that the temporal decoupling of clustering and transcription might not be a unique case. First, we observed that numerous small Pol II clusters away from the histone locus also lack visible Ser2ph enrichment (fig. S4 and movie S3). Second, artificially induced clustering of sequence-specific transcription factors does not necessarily lead to a corresponding increase in transcription (*20*, *21*). Third, a recent study showed that only a fraction of Notch transcription hubs become transcriptionally active upon signaling (*59*), suggesting that the stepwise control mechanism we observed here may apply to other components of the transcription machinery besides Pol II.

The Integrator endonuclease is required for the promoter-proximal termination of many genes (*51–54*, *60*) but whether it ultimately activates (*53*, *61–63*) or represses (*64*, *65*) transcription has been a subject of debate. Recent genome-wide analyses (*54*, *66*) revealed differential effects across various protein-coding genes upon depleting IntS11, with highly expressed genes showing downregulation and lowly expressed genes showing upregulation (*54*) Consistent with this nuanced picture, loss of IntS11 leads to up-regulation of histone expression in G-phase and down-regulation in S-phase. This bivalent outcome suggests that IntS11-mediated clustering could function similarly to a dam, blocking Pol II from transitioning into active elongation when its control gates are shut (G-phase), in the process accumulating a large pool of Pol II poised for rapid activation when the signal to open the gates is received in S-phase. Depletion of IntS11 thus results in both a loss of the transcription blockade in G-phase, as well as lowered activation in S-phase because the system was unable to build up enough Pol II reserves. If general, this model of Integrator regulation might similarly explain the down-regulation of highly active genes (where the control gates are supposedly open) and the up-regulation of lowly active genes (where the control gates are supposedly shut) upon IntS11 perturbation.

Finally, we observe that clustered Pol II molecules spend substantial periods in a poised state. Poised genes have long been proposed to be regulated by promoter-proximal pausing of Pol II (*67–73*). While HLBs contain both unbound and paused Pol II molecules, depletion of pausing factors Spt6 and Spt5 did not result in leaky histone expression, suggesting that promoter-proximal pausing alone is insufficient to maintain the poised state. In summary, our study presents evidence that Pol II clustering plays multifaceted roles in transcription and sheds light on Integrator functions as well as promoter-proximal regulation.

Acknowledgments: We thank Robert Duronio (UNC-Chapel Hill) for the GFP-mxc fly line and anti-Mxc antibody, Elizabeth Gavis (Princeton) for the GFP-CycE fly line, Akira Nakamura (RIKEN) for anti-CycT antibody, John Lis (Cornell) for anti-Spt6 antibody, Stefano Di Talia (Duke) for discussion on the DS-H3 HCR FISH probe design, Luke Lavis (Janelia) for the JF dyes. Eric Wagner (URMC), Yu Cai (NUS), and Patrick O'Farrell (UCSF) for critical reagents, Yujun Chen (K-State) for *ex-vivo* ovary culture advice, Nicholas Mamrak for designing the 5'- and 3'-H3 HCR FISH probes, Chengye Feng (Yale) for FRAP analysis advice, Eli Rothenberg's lab (NYU Langone) for assistance with EU labeling, NYU Langone Health Microscopy Laboratory (RRID: SCR_017934) Michael Cammer and Yan Deng for consultation and assistance with optical microscopy services, the TRiP at Harvard Medical School for providing various RNAi fly stocks used in this study, the Lionnet and Lehmann lab members for comments.

Funding:

National Institutes of Health grant R01 AG075272 to T.L.

National Institutes of Health grant R01 HD110546-01 to R.L.

National Institutes of Health grant R01 GM047477 to D.S.G.

National Institutes of Health grant R35 GM119735 to J.E.W.

Cancer Prevention & Research Institute of Texas grant RR210031 to J.E.W. J.E.W. is a CPRIT Scholar Cancer Research.

Microscopy shared resource is partially supported by the Cancer Center Support Grant, P30CA016087.

NYSTEM Institutional Training Grant #C032560GG to F.L.

Author contributions: F.L. conceived the project. T.L. and R.L. co-supervised the project. F.L., R.L., and T.L. designed experiments. B.J.P. performed Pol II CTD mutational analyses and contributed to crucial preliminary data. R.F. and J.E.W. designed and generated the *Drosophila* IntS8 antibody. D.S.G. generated the Halo-Rpb1 fly line and supported the initial phase of the project. F.L. performed all other experiments. F.L. and T.L. analyzed the data. F.L., R.L., and T.L. interpreted the data. F.L. drafted the manuscript. F.L. T.L., R.L., D.S.G., J.E.W., and B.J.P. revised the manuscript.

Competing interests: Authors declare that they have no competing interests.

Data and materials availability: All data are available in the main text or the supplementary materials.

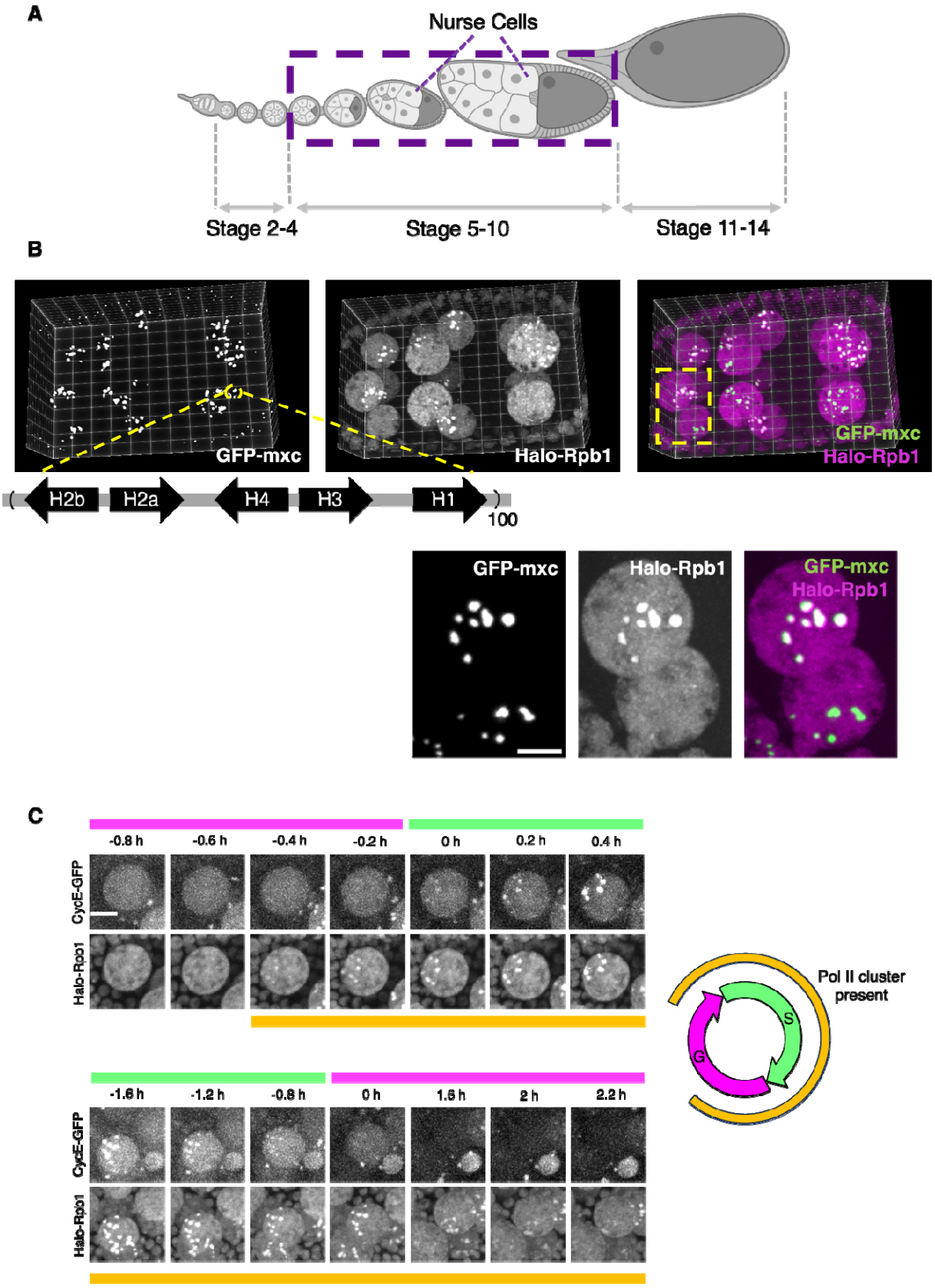
A
Nurse Cells
Stage 2-4
Stage 5-10
Stage 11-14
B
GFP-mxc
Halo-Rpb1
GFP-mxc
Halo-Rpb1
H2b
H2a
H4
H3
H1
100
GFP-mxc
Halo-Rpb1
GFP-mxc
Halo-Rpb1
C
-0.8 h
-0.6 h
-0.4 h
-0.2 h
0 h
0.2 h
0.4 h
CycE-GFP
Halo-Rpb1
-1.6 h
-1.2 h
-0.8 h
0 h
1.6 h
2 h
2.2 h
CycE-GFP
Halo-Rpb1
Pol II cluster
present
S
G

Fig. 1. Micron-sized Pol II clusters are present at HLBs of the *Drosophila* NCs both during and outside of the S-phase. (**A**) A schematic of a developing ovariole, which contains egg chambers of increasing maturity from anterior to posterior. Each egg chamber consists of 15 NCs and an oocyte (dark gray). All experiments in this study are performed in NCs between Stages 5 and 10 (boxed region) when the nuclei grow from 10 µm to above 50 µm in diameter. (**B**) Upper: 3D rendering of a Stage 6 egg chamber expressing the HLB marker GFP-mxc and Halo-tagged Rpb1. Lower: Z projection of the boxed region in the upper panel showing two nuclei, one of which has distinct Pol II clusters present at HLBs. The scale bar represents 5 µm. (**C**) Time-lapse movies of two nuclei that are entering (upper) and exiting (lower) the S-phase respectively. CycE-GFP is a cell-cycle marker (*33*). See also fig. S2. Time 0 represents the start of the S-phase (upper) and the G-phase (lower) respectively. Halo-Rpb1 was labeled by Janelia Fluor 549 (JF549) (*74*). The scale bar represents 10 µm.

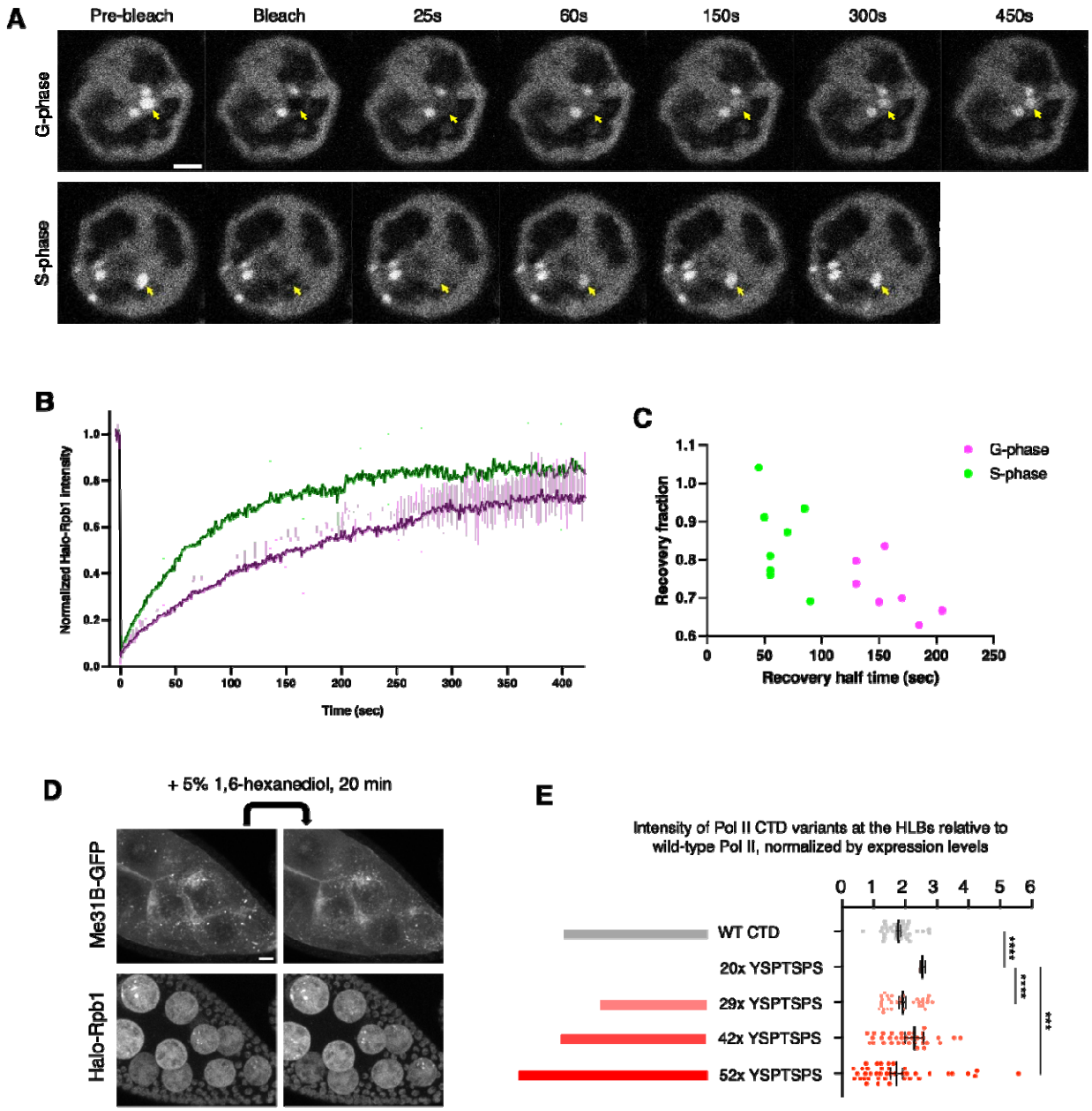

Fig. 2. The HLB-bound Pol II clusters show slow recovery in FRAP, are insensitive to hexanediol, and do not show more clustering at increased CTD lengths. (**A**) Two examples of FRAP experiments targeting HLB-bound Pol II clusters. The yellow arrows indicate bleached clusters. The upper G-phase cluster showed only partial recovery after 450 seconds whereas the lower S-phase cluster showed near full recovery after 150 seconds. Halo-Rpb1 was labeled by Janelia Fluor 552 (JF552) (*75*). The scale bar represents 5 µm. (**B**) Normalized FRAP curves of G-phase (magenta) and S-phase (green) HLB-bound Pol II clusters. The black lines represent the averages of data acquired from 7 G-phase and 8 S-phase nuclei derived from a total of 4 ovaries. The vertical colored lines represent the ranges. (**C**) Scatter plot of the half-recovery time and the recovered fraction of 7 G-phase and 8 S-phase nuclei. (**D**) Treatment with 5% 1,6-hexanediol for

20 min dissolves P-bodies (marked by Me31B-GFP) but not Pol II clusters. The scale bar represents 10 µm. (**E**) Normalized intensity of Pol II CTD variants at HLBs. Each dot represents the ratio of FLAG-tagged Pol II CTD variants to HA-tagged wild-type (WT) Pol II at HLBs, averaged across one nucleus (normalized by expression). The WT *Drosophila* Pol II CTD contains 42 repeats, most of which are variants of the consensus YSPTSPS motif. Pol II CTD variants contain 20, 29, 42, and 52 precise copies of YSPTSPS (*44*). Error bars represent mean ± SEM. Data was acquired from at least 4 female flies per genotype. ***P<0.001 and ****P<0.0001. See also Materials and Methods and fig. S3.

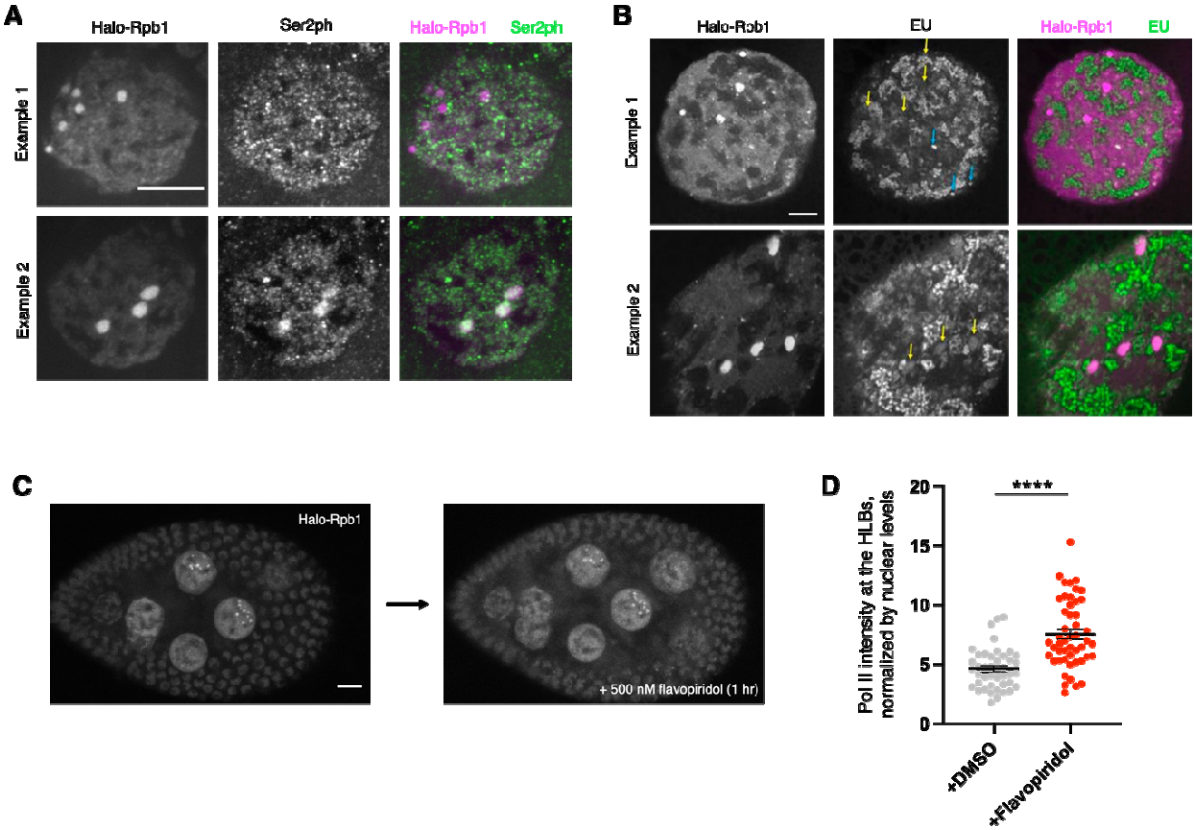

Fig. 3. Most HLB-bound Pol II clusters lack detectable levels of Ser2ph and EU and are not dispersed when elongation is inhibited. (**A**) Representative images of HLB-bound Pol II clusters scored negative (Example 1) or positive (Example 2) for Ser2ph staining. (**B**) Representative images of HLB-bound Pol II clusters scored negative (Example 1) or positive (Example 2) for EU incorporation. HLBs are marked by yellow arrows; blue arrows mark small EU-rich foci. Nucleoli (nuclear regions with low Pol II intensity) also showed strong EU enrichment consistent with their role in rRNA synthesis. (**C**) The HLB-bound Pol II clusters survived a 1-hour treatment with 500 nM FP. Halo-Rpb1 was labeled by Janelia Fluor 646 (JF646) (*74*). (**D**) Quantification of the levels of Pol II at HLBs in DMSO- versus FP-treated egg chambers. Each dot represents one NC. Error bars represent mean ± SEM. All data was stage-

matched and acquired from at least 6 female flies per condition. ****P<0.0001. Scale bars represent 10 µm.

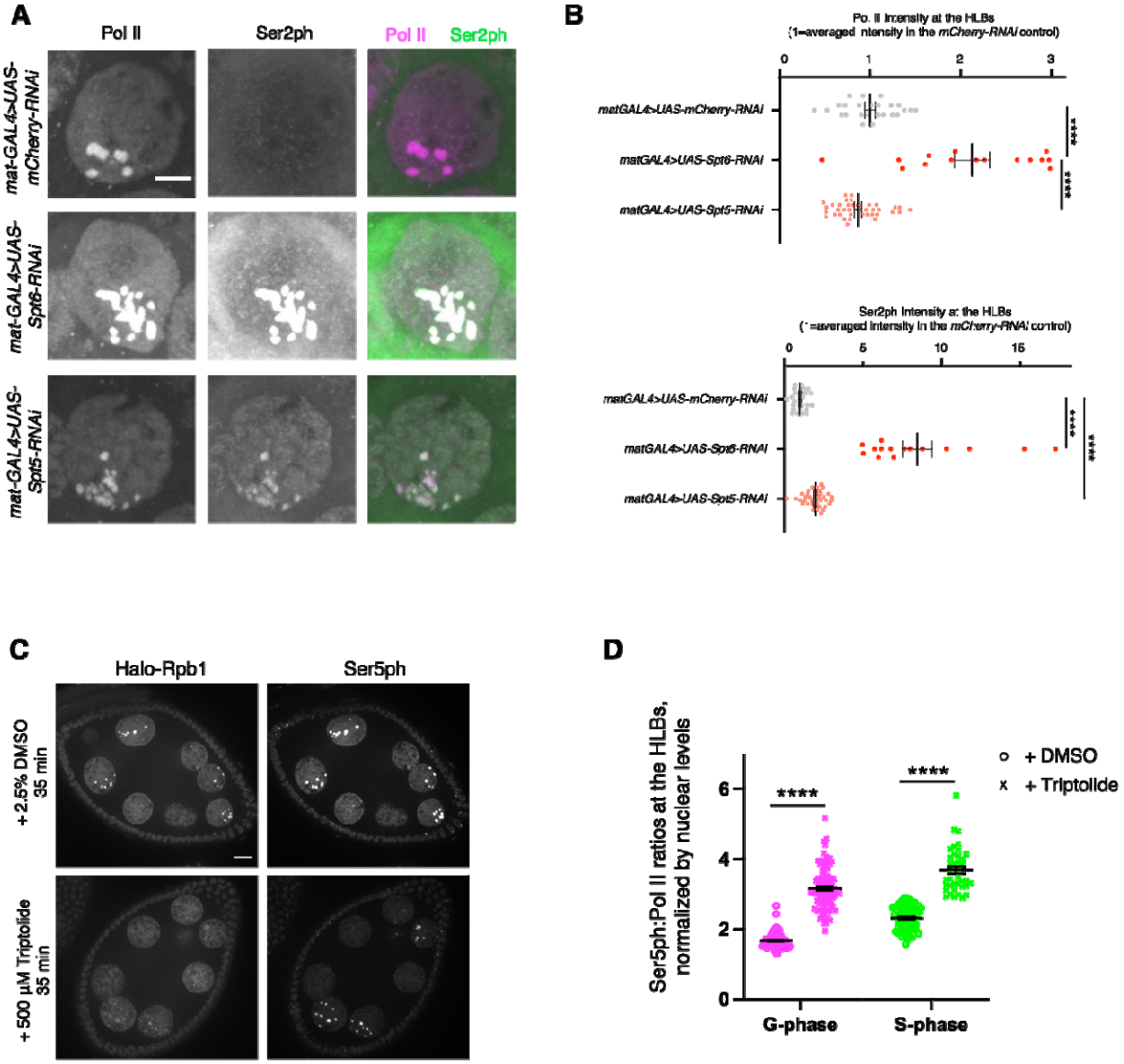

Fig. 4. Both promoter-proximal paused and unbound Pol II molecules are present at the HLB-bound clusters. (**A**) RNAi depletion of Spt6 and Spt5 results in increased levels of Ser2ph at HLBs. mCherry-RNAi serves as a negative control. The scale bar represents 5 µm. (**B**) Quantification of Pol II (upper) and Ser2ph (lower) levels at HLBs. Each dot represents one NC. The increased levels of Ser2ph are not explained by levels of Pol II at HLBs. Spt6 RNAi: 8.45±0.96 (Ser2ph) versus 2.12±0.19 (Pol II); Spt5 RNAi: 1.95±0.10 (Ser2ph) versus 0.87±0.04 (Pol II). Error bars represent mean ± SEM. Data was collected from 11, 5, and 6 egg chambers (from at least 3 females per genotype) for mCherry RNAi, Spt6 RNAi, and Spt5 RNAi respectively. ****P<0.0001. (**C**) 35 min of 500 µM TRI treatment results in decreased levels of

Pol II and Ser5ph at HLBs. Halo-Rpb1 was labeled by JF646. The scale bar represents 10 µm. (**D**) Quantification of the Ser5ph:Pol II ratios at HLBs in DMSO-treated versus TRI-treated NCs, grouped by cell cycle stages. Each dot represents the average Ser5ph:Pol II ratio in one nucleus. Error bars represent mean ± SEM. Data was stage-matched and acquired from at least 6 female flies per condition. The levels of Ser5ph and Pol II were normalized by their nuclear levels. ****P<0.0001. See also Materials and Methods and fig. S8.

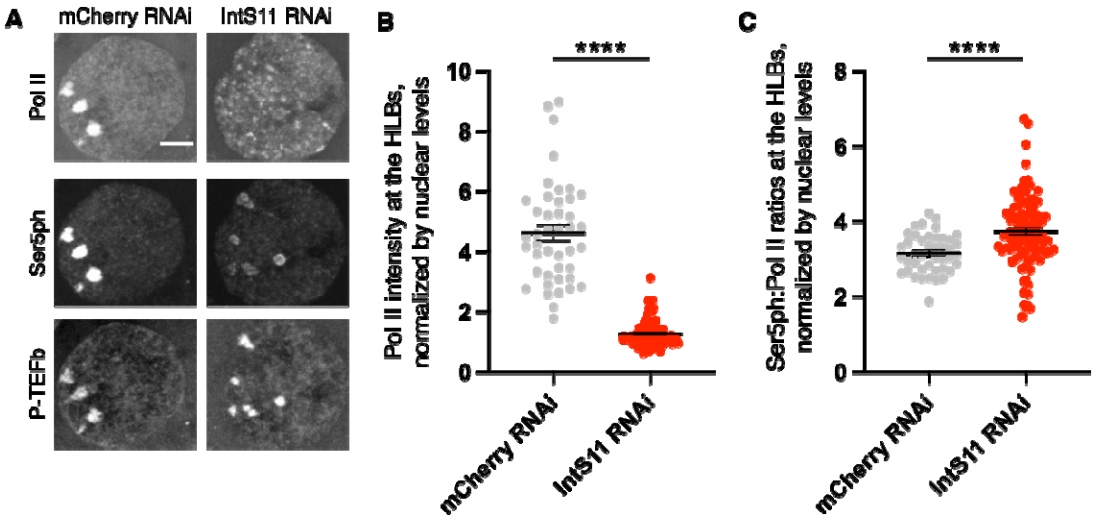

Fig. 5. Depletion of IntS11 eliminates all HLB-bound Pol II clusters, which can be partially restored by inhibiting P-TEFb. (**A**) RNAi depletion of IntS11 results in complete loss of Pol II clusters at HLBs. P-TEFb is enriched at HLBs during the S-phase (see also fig. S11), which serves as a cell cycle marker. mCherry-RNAi serves as a negative control. The scale bar represents 5 µm. (**B** and **C**) Quantification of the levels of Pol II (B) and Ser5ph:Pol II ratios (C) at the S-phase HLBs (demarcated by MPM-2). Each dot represents one NC. Error bars represent mean ± SEM. All data was stage-matched and acquired from at least 6 female flies per condition. The levels of Ser5ph and Pol II were normalized by their nuclear levels. ****P<0.0001. See also Materials and Methods.

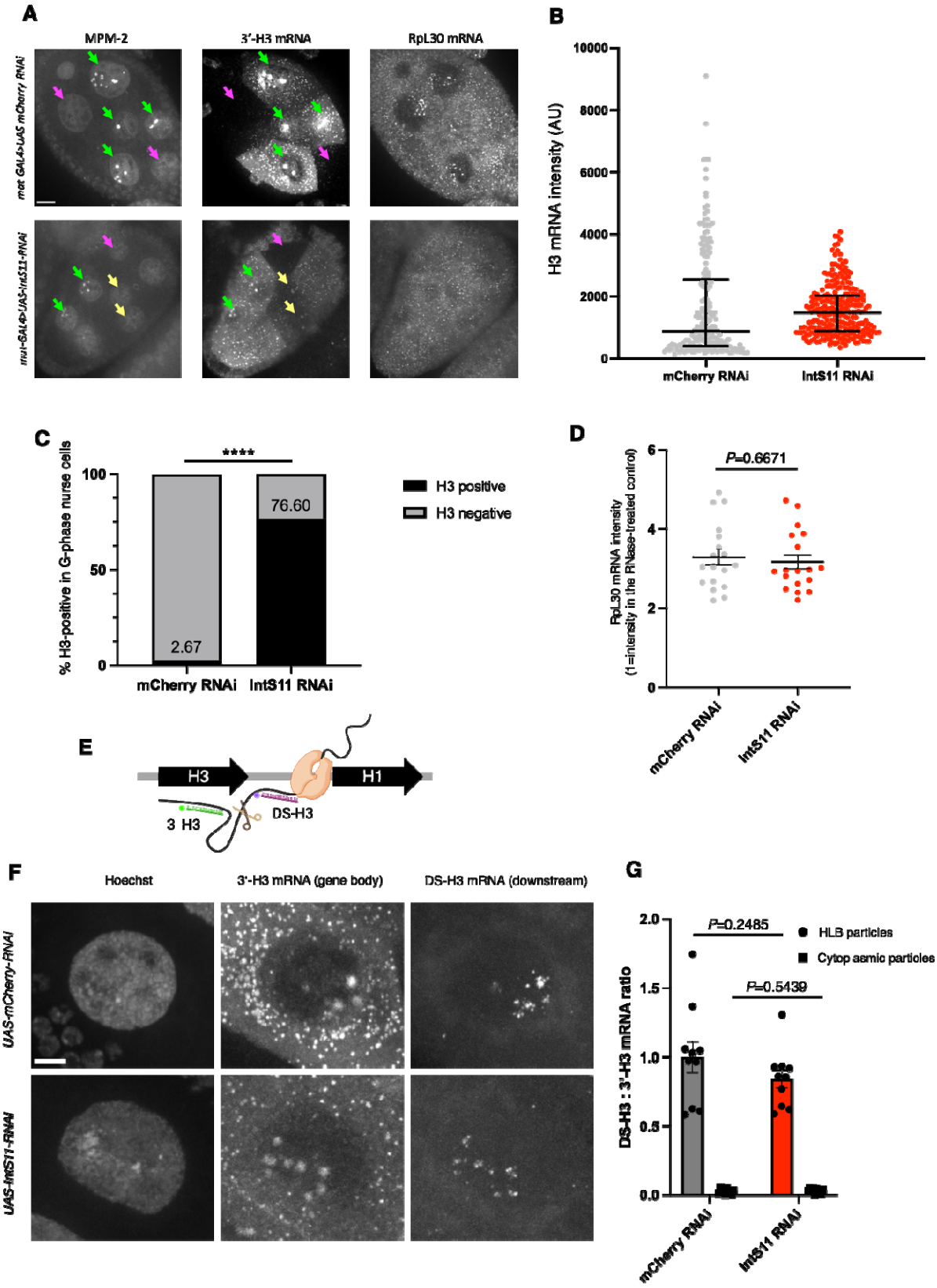
A
MPM-2
3'-H3 mRNA
RpL30 mRNA
mat GAL4>UAS mCherry RNAi
mat-GAL4>UAS-IntS11-RNAi
B
H3 mRNA intensity (AU)
10000
8000
6000
4000
2000
0
mCherry RNAi
IntS11 RNAi
C
% H3-positive in G-phase nurse cells
****
100
50
0
2.67
76.60
H3 positive
H3 negative
mCherry RNAi
IntS11 RNAi
D
RpL30 mRNA intensity
(1=intensity in the RNase-treated control)
P=0.6671
6
4
2
0
mCherry RNAi
IntS11 RNAi
E
H3
H1
3 H3
DS-H3
F
Hoechst
3'-H3 mRNA (gene body)
DS-H3 mRNA (downstream)
mat-GAL4>
UAS-mCherry-RNAi
mat-GAL4>
UAS-IntS11-RNAi
G
DS-H3 : 3'-H3 mRNA ratio
P=0.2485
P=0.5439
HLB particles
Cytoplasmic particles
2.0
1.5
1.0
0.5
0.0
mCherry RNAi
IntS11 RNAi

Fig. 6. Depletion of IntS11 results in reduced induction and out-of-phase histone transcription. (**A**) Representative images showing egg chambers probed with MPM-2 (S-phase marker), 3'-H3 mRNA, and RpL30 mRNA (control). mCherry-RNAi serves as a negative control. Green arrows point at the S-phase NCs whereas magenta and yellow arrows point at the G-phase NCs without and with H3 mRNA respectively. (**B**) Quantification of the cytoplasmic H3 mRNA intensity. Each dot represents one NC. Bars represent quartiles. $P<0.00001$ estimated by bootstrapping of the 10th and 90th percentiles. (**C**) Quantification of % of MPM-2 negative NCs with cytoplasmic H3 mRNA signals. n=75 (*mCherry-RNAi*), n=94 (*IntS11-RNAi*). Two-sided chi-square test. See also fig. S16. (**D**) Quantification of cytoplasmic RpL30 mRNA. Each dot represents the average mRNA level in one egg chamber. Error bars represent mean ± SEM. ****$P<0.0001$. (**E**) A schematic showing the design of downstream H3 (DS-H3) probe for detection of unprocessed H3 mRNA, adapted from (*36*). (**F**) Representative images showing NCs probed with both the 3'-H3 and DS-H3 FISH probes. DNA was detected by Hoechst as a reference for the nuclei. (**G**) Quantification of DS-H3 to 3'-H3 mRNA ratios at HLBs and the mRNA clusters in the cytoplasm. Each dot represents one NC. Error bars represent mean ± SEM. All data was stage-matched and acquired from at least 6 female flies per genotype. Scale bars represent 10 µm.

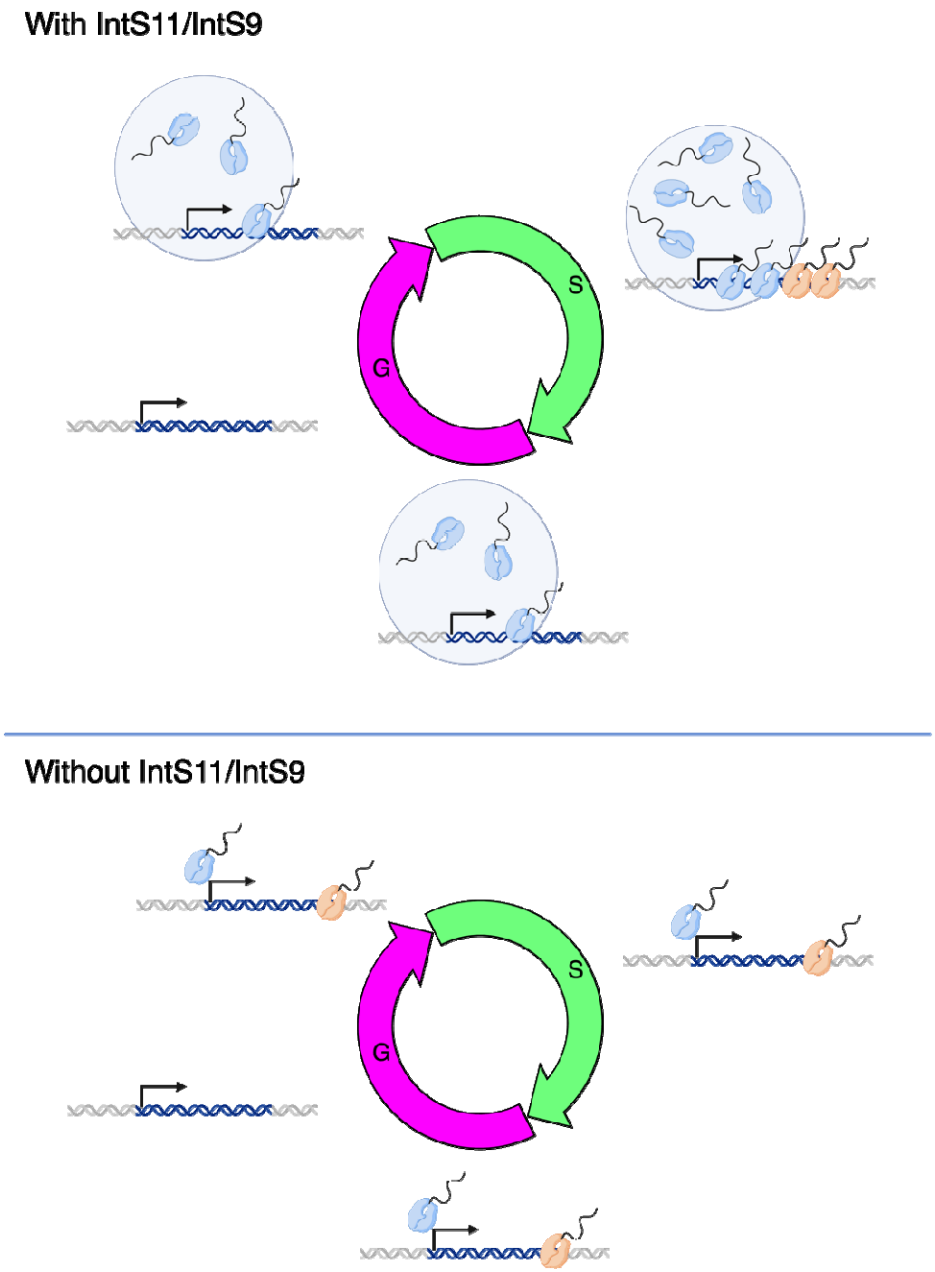

Fig. 7. Model for clustering-regulated transcription at the replication-dependent histone genes. Poised and elongating Pol II molecules are marked in blue and orange respectively. Normally, Pol II molecules start to form clusters during the G-phase and remain inactive near promoters until they are licensed for transcription during the S-phase. In the absence of the Integrator endonuclease, clustering-regulated transcription is lost. As a result, Pol II becomes elongation-competent once recruited to the promoters, leading to “leaky” histone transcription in G-phase as well as reduced histone transcription induction in S-phase.

References

1. I. I. Cisse, I. Izeddin, S. Z. Causse, L. Boudarene, A. Senecal, L. Muresan, C. Dugast-Darzacq, B. Hajj, M. Dahan, X. Darzacq, Real-Time Dynamics of RNA Polymerase II Clustering in Live Human Cells. *Science*. **341** (2013), pp. 664–667.

2. W.-K. Cho, N. Jayanth, B. P. English, T. Inoue, J. O. Andrews, W. Conway, J. B. Grimm, J.-H. Spille, L. D. Lavis, T. Lionnet, I. I. Cisse, RNA Polymerase II cluster dynamics predict mRNA output in living cells. *Elife*. **5** (2016), doi:10.7554/eLife.13617.

3. W.-K. Cho, J.-H. Spille, M. Hecht, C. Lee, C. Li, V. Grube, I. I. Cisse, Mediator and RNA polymerase II clusters associate in transcription-dependent condensates. *Science* (2018), doi:10.1126/science.aar4199.

4. Y. E. Guo, J. C. Manteiga, J. E. Henninger, B. R. Sabari, A. Dall'Agnese, N. M. Hannett, J.-H. Spille, L. K. Afeyan, A. V. Zamudio, K. Shrinivas, B. J. Abraham, A. Boija, T.-M. Decker, J. K. Rimel, C. B. Fant, T. I. Lee, I. I. Cisse, P. A. Sharp, D. J. Taatjes, R. A. Young, Pol II phosphorylation regulates a switch between transcriptional and splicing condensates. *Nature*. **572**, 543–548 (2019).

5. J. Li, A. Dong, K. Saydaminova, H. Chang, G. Wang, H. Ochiai, T. Yamamoto, A. Pertsinidis, Single-Molecule Nanoscopy Elucidates RNA Polymerase II Transcription at Single Genes in Live Cells. *Cell*. **178**, 491–506.e28 (2019).

6. S.-K. Huang, P. H. Whitney, S. Dutta, S. Y. Shvartsman, C. A. Rushlow, Spatial organization of transcribing loci during early genome activation in Drosophila. *Curr. Biol.* **31**, 5102–5110.e5 (2021).

7. V. Q. Nguyen, A. Ranjan, S. Liu, X. Tang, Y. H. Ling, J. Wisniewski, G. Mizuguchi, K. Y. Li, V. Jou, Q. Zheng, L. D. Lavis, T. Lionnet, C. Wu, Spatiotemporal coordination of transcription preinitiation complex assembly in live cells. *Mol. Cell*. **81**, 3560–3575.e6 (2021).

8. T. Imada, T. Shimi, A. Kaiho, Y. Saeki, H. Kimura, RNA polymerase II condensate formation and association with Cajal and histone locus bodies in living human cells. *Genes Cells*. **26**, 298–312 (2021).

9. C.-Y. Cho, J. P. Kemp Jr, R. J. Duronio, P. H. O'Farrell, Coordinating transcription and replication to mitigate their conflicts in early Drosophila embryos. *Cell Rep.* **41**, 111507 (2022).

10. B. R. Sabari, A. Dall'Agnese, A. Boija, I. A. Klein, E. L. Coffey, K. Shrinivas, B. J. Abraham, N. M. Hannett, A. V. Zamudio, J. C. Manteiga, C. H. Li, Y. E. Guo, D. S. Day, J. Schuijers, E. Vasile, S. Malik, D. Hnisz, T. I. Lee, I. I. Cisse, R. G. Roeder, P. A. Sharp, A. K. Chakraborty, R. A. Young, Coactivator condensation at super-enhancers links phase separation and gene control. *Science*. **361** (2018), doi:10.1126/science.aar3958.

11. H. Lu, D. Yu, A. S. Hansen, S. Ganguly, R. Liu, A. Heckert, X. Darzacq, Q. Zhou, Phase-

separation mechanism for C-terminal hyperphosphorylation of RNA polymerase II. *Nature*. **558**, 318–323 (2018).

12. P. Rawat, M. Boehning, B. Hummel, F. Aprile-Garcia, A. S. Pandit, N. Eisenhardt, A. Khavaran, E. Niskanen, S. M. Vos, J. J. Palvimo, A. Pichler, P. Cramer, R. Sawarkar, Stress-induced nuclear condensation of NELF drives transcriptional downregulation. *Mol. Cell*. **81**, 1013–1026.e11 (2021).

13. M. Mir, A. Reimer, J. E. Haines, X.-Y. Li, M. Stadler, H. Garcia, M. B. Eisen, X. Darzacq, Dense Bicoid hubs accentuate binding along the morphogen gradient. *Genes Dev*. **31**, 1784–1794 (2017).

14. S. Chong, C. Dugast-Darzacq, Z. Liu, P. Dong, G. M. Dailey, C. Cattoglio, A. Heckert, S. Banala, L. Lavis, X. Darzacq, R. Tjian, Imaging dynamic and selective low-complexity domain interactions that control gene transcription. *Science*. **361** (2018), doi:10.1126/science.aar2555.

15. M. Mir, M. R. Stadler, S. A. Ortiz, C. E. Hannon, M. M. Harrison, X. Darzacq, M. B. Eisen, Dynamic multifactor hubs interact transiently with sites of active transcription in Drosophila embryos. *Elife*. **7** (2018), doi:10.7554/eLife.40497.

16. F. Lu, T. Lionnet, Transcription Factor Dynamics. *Cold Spring Harb. Perspect. Biol.* **13** (2021), doi:10.1101/cshperspect.a040949.

17. A. Boija, I. A. Klein, B. R. Sabari, A. Dall'Agnese, E. L. Coffey, A. V. Zamudio, C. H. Li, K. Shrinivas, J. C. Manteiga, N. M. Hannett, B. J. Abraham, L. K. Afeyan, Y. E. Guo, J. K. Rimel, C. B. Fant, J. Schuijers, T. I. Lee, D. J. Taatjes, R. A. Young, Transcription Factors Activate Genes through the Phase-Separation Capacity of Their Activation Domains. *Cell*. **175**, 1842–1855.e16 (2018).

18. H. Lyons, R. T. Veettil, P. Pradhan, C. Fornero, N. De La Cruz, K. Ito, M. Eppert, R. G. Roeder, B. R. Sabari, Functional partitioning of transcriptional regulators by patterned charge blocks. *Cell*. **186**, 327–345.e28 (2023).

19. D. T. McSwiggen, A. S. Hansen, S. S. Teves, H. Marie-Nelly, Y. Hao, A. B. Heckert, K. K. Umemoto, C. Dugast-Darzacq, R. Tjian, X. Darzacq, Evidence for DNA-mediated nuclear compartmentalization distinct from phase separation. *Elife*. **8** (2019), doi:10.7554/eLife.47098.

20. J. Trojanowski, L. Frank, A. Rademacher, N. Mücke, P. Grigaitis, K. Rippe, Transcription activation is enhanced by multivalent interactions independent of phase separation. *Mol. Cell*. **82**, 1878–1893.e10 (2022).

21. S. Chong, T. G. W. Graham, C. Dugast-Darzacq, G. M. Dailey, X. Darzacq, R. Tjian, Tuning levels of low-complexity domain interactions to modulate endogenous oncogenic transcription. *Mol. Cell*. **82**, 2084–2097.e5 (2022).

22. A. J. Plys, R. E. Kingston, Dynamic condensates activate transcription. *Science*. **361** (2018),

pp. 329–330.

23. M.-T. Wei, Y.-C. Chang, S. F. Shimobayashi, Y. Shin, A. R. Strom, C. P. Brangwynne, Nucleated transcriptional condensates amplify gene expression. *Nat. Cell Biol.* **22**, 1187–1196 (2020).

24. N. Schneider, F.-G. Wieland, D. Kong, A. A. M. Fischer, M. Hörner, J. Timmer, H. Ye, W. Weber, Liquid-liquid phase separation of light-inducible transcription factors increases transcription activation in mammalian cells and mice. *Sci Adv*. **7** (2021), doi:10.1126/sciadv.abd3568.

25. Y. J. Kim, M. Lee Jr, Y.-T. Lee, J. Jing, J. T. Sanders, G. A. Botten, L. He, J. Lyu, Y. Zhang, M. Mettlen, P. Ly, Y. Zhou, J. Xu, Light-activated macromolecular phase separation modulates transcription by reconfiguring chromatin interactions. *Sci Adv*. **9**, eadg1123 (2023).

26. I. Kwon, M. Kato, S. Xiang, L. Wu, P. Theodoropoulos, H. Mirzaei, T. Han, S. Xie, J. L. Corden, S. L. McKnight, Phosphorylation-regulated binding of RNA polymerase II to fibrous polymers of low-complexity domains. *Cell*. **155**, 1049–1060 (2013).

27. M. Boehning, C. Dugast-Darzacq, M. Rankovic, A. S. Hansen, T. Yu, H. Marie-Nelly, D. T. McSwiggen, G. Kokic, G. M. Dailey, P. Cramer, X. Darzacq, M. Zweckstetter, RNA polymerase II clustering through carboxy-terminal domain phase separation. *Nat. Struct. Mol. Biol.* (2018), doi:10.1038/s41594-018-0112-y.

28. K. M. Harlen, L. S. Churchman, The code and beyond: transcription regulation by the RNA polymerase II carboxy-terminal domain. *Nat. Rev. Mol. Cell Biol.* **18**, 263–273 (2017).

29. P. Quintero-Cadena, T. L. Lenstra, P. W. Sternberg, RNA Pol II Length and Disorder Enable Cooperative Scaling of Transcriptional Bursting. *Mol. Cell*. **79**, 207–220.e8 (2020).

30. D. Eick, M. Geyer, The RNA polymerase II carboxy-terminal domain (CTD) code. *Chem. Rev*. **113**, 8456–8490 (2013).

31. J. L. Corden, RNA polymerase II C-terminal domain: Tethering transcription to transcript and template. *Chem. Rev*. **113**, 8423–8455 (2013).

32. J. Zaborowska, S. Egloff, S. Murphy, The pol II CTD: new twists in the tail. *Nat. Struct. Mol. Biol.* **23**, 771–777 (2016).

33. C. A. Doherty, R. Diegmiller, M. Kapasiawala, E. R. Gavis, S. Y. Shvartsman, Coupled oscillators coordinate collective germline growth. *Dev. Cell*. **56**, 860–870.e8 (2021).

34. B. Guglielmi, N. La Rochelle, R. Tjian, Gene-specific transcriptional mechanisms at the histone gene cluster revealed by single-cell imaging. *Mol. Cell*. **51**, 480–492 (2013).

35. D. J. McKay, S. Klusza, T. J. R. Penke, M. P. Meers, K. P. Curry, S. L. McDaniel, P. Y. Malek, S. W. Cooper, D. C. Tatomer, J. D. Lieb, B. D. Strahl, R. J. Duronio, A. G. Matera,

Interrogating the function of metazoan histones using engineered gene clusters. *Dev. Cell*. **32**, 373–386 (2015).

36. W. Hur, J. P. Kemp Jr, M. Tarzia, V. E. Deneke, W. F. Marzluff, R. J. Duronio, S. Di Talia, CDK-Regulated Phase Separation Seeded by Histone Genes Ensures Precise Growth and Function of Histone Locus Bodies. *Dev. Cell*. **54**, 379–394.e6 (2020).

37. Z. F. Nizami, S. Deryusheva, J. G. Gall, Cajal bodies and histone locus bodies in Drosophila and Xenopus. *Cold Spring Harb. Symp. Quant. Biol.* **75**, 313–320 (2010).

38. J.-L. Liu, C. Murphy, M. Buszczak, S. Clatterbuck, R. Goodman, J. G. Gall, The Drosophila melanogaster Cajal body. *J. Cell Biol.* **172**, 875–884 (2006).

39. J. M. Potter-Birriel, G. B. Gonsalvez, W. F. Marzluff, A region of SLBP outside the mRNA-processing domain is essential for deposition of histone mRNA into the Drosophila egg. *J. Cell Sci.* **134** (2021), doi:10.1242/jcs.251728.

40. F. Lu, D. S. Gilmour, Genetic analysis of the RNA polymerase II CTD in Drosophila. *Methods*. **159-160**, 129–137 (2019).

41. C. Armstrong, V. J. Passanisi, H. M. Ashraf, S. L. Spencer, Cyclin E/CDK2 and feedback from soluble histone protein regulate the S phase burst of histone biosynthesis. *Cell Rep.* **42**, 112768 (2023).

42. J. Yao, M. B. Ardehali, C. J. Fecko, W. W. Webb, J. T. Lis, Intranuclear distribution and local dynamics of RNA polymerase II during transcription activation. *Mol. Cell*. **28**, 978–990 (2007).

43. M. Sankaranarayanan, R. J. Emenecker, E. L. Wilby, M. Jahnel, I. R. E. A. Trussina, M. Wayland, S. Alberti, A. S. Holehouse, T. T. Weil, Adaptable P body physical states differentially regulate bicoid mRNA storage during early Drosophila development. *Dev. Cell*. **56**, 2886–2901.e6 (2021).

44. F. Lu, B. Portz, D. S. Gilmour, The C-Terminal Domain of RNA Polymerase II Is a Multivalent Targeting Sequence that Supports Drosophila Development with Only Consensus Heptads. *Mol. Cell*. **73**, 1232–1242.e4 (2019).

45. C. Y. Jao, A. Salic, Exploring RNA transcription and turnover in vivo by using click chemistry. *Proc. Natl. Acad. Sci. U. S. A.* **105**, 15779–15784 (2008).

46. S. H. Chao, D. H. Price, Flavopiridol inactivates P-TEFb and blocks most RNA polymerase II transcription in vivo. *J. Biol. Chem.* **276**, 31793–31799 (2001).

47. K. Fujinaga, F. Huang, B. M. Peterlin, P-TEFb: The master regulator of transcription elongation. *Mol. Cell*. **83**, 393–403 (2023).

48. Y. Aoi, A. P. Shah, S. Ganesan, S. H. A. Soliman, B.-K. Cho, Y. A. Goo, N. L. Kelleher, A. Shilatifard, SPT6 functions in transcriptional pause/release via PAF1C recruitment. *Mol.*

Cell. **82**, 3412–3423.e5 (2022).

49. N. Fong, R. M. Sheridan, S. Ramachandran, D. L. Bentley, The pausing zone and control of RNA polymerase II elongation by Spt5: Implications for the pause-release model. *Mol. Cell*. **82**, 3632–3645.e4 (2022).

50. W. Shao, J. Zeitlinger, Paused RNA polymerase II inhibits new transcriptional initiation. *Nat. Genet.* **49**, 1045–1051 (2017).

51. S. A. Welsh, A. Gardini, Genomic regulation of transcription and RNA processing by the multitasking Integrator complex. *Nat. Rev. Mol. Cell Biol.* **24**, 204–220 (2023).

52. E. J. Wagner, L. Tong, K. Adelman, Integrator is a global promoter-proximal termination complex. *Mol. Cell*. **83**, 416–427 (2023).

53. H. Wang, Z. Fan, P. V. Shliaha, M. Miele, R. C. Hendrickson, X. Jiang, K. Helin, Publisher Correction: H3K4me3 regulates RNA polymerase II promoter-proximal pause-release. *Nature*. **616**, E7 (2023).

54. S. Hu, L. Peng, A. Song, Y.-X. Ji, J. Cheng, M. Wang, F. X. Chen, INTAC endonuclease and phosphatase modules differentially regulate transcription by RNA polymerase II. *Mol. Cell*. **83**, 1588–1604.e5 (2023).

55. I. Fianu, Y. Chen, C. Dienemann, O. Dybkov, A. Linden, H. Urlaub, P. Cramer, Structural basis of Integrator-mediated transcription regulation. *Science*. **374**, 883–887 (2021).

56. H. Zheng, Y. Qi, S. Hu, X. Cao, C. Xu, Z. Yin, X. Chen, Y. Li, W. Liu, J. Li, J. Wang, G. Wei, K. Liang, F. X. Chen, Y. Xu, Identification of Integrator-PP2A complex (INTAC), an RNA polymerase II phosphatase. *Science*. **370** (2020), doi:10.1126/science.abb5872.

57. W. F. Marzluff, E. J. Wagner, R. J. Duronio, Metabolism and regulation of canonical histone mRNAs: life without a poly(A) tail. *Nat. Rev. Genet.* **9**, 843–854 (2008).

58. A. Papantonis, P. R. Cook, Transcription factories: genome organization and gene regulation. *Chem. Rev.* **113**, 8683–8705 (2013).

59. F. Javier deHaro-Arbona, C. Roussos, S. Baloul, J. Townson, M. J. Gomez-Lamarca, S. Bray, Dynamic modes of Notch transcription hubs conferring memory and stochastic activation revealed by live imaging the co-activator Mastermind. *bioRxiv* (2023), p. 2023.08.10.552629.

60. M. S. Mendoza-Figueroa, D. C. Tatomer, J. E. Wilusz, The Integrator Complex in Transcription and Development. *Trends Biochem. Sci.* **45**, 923–934 (2020).

61. A. Gardini, D. Baillat, M. Cesaroni, D. Hu, J. M. Marinis, E. J. Wagner, M. A. Lazar, A. Shilatifard, R. Shiekhattar, Integrator regulates transcriptional initiation and pause release following activation. *Mol. Cell*. **56**, 128–139 (2014).

62. B. Stadelmayer, G. Micas, A. Gamot, P. Martin, N. Malirat, S. Koval, R. Raffel, B. Sobhian, D. Severac, S. Rialle, H. Parrinello, O. Cuvier, M. Benkirane, Integrator complex regulates NELF-mediated RNA polymerase II pause/release and processivity at coding genes. *Nat. Commun.* **5**, 5531 (2014).

63. F. Beckedorff, E. Blumenthal, L. F. daSilva, Y. Aoi, P. R. Cingaram, J. Yue, A. Zhang, S. Dokaneheifard, M. G. Valencia, G. Gaidosh, A. Shilatifard, R. Shiekhattar, The Human Integrator Complex Facilitates Transcriptional Elongation by Endonucleolytic Cleavage of Nascent Transcripts. *Cell Rep.* **32**, 107917 (2020).

64. N. D. Elrod, T. Henriques, K.-L. Huang, D. C. Tatomer, J. E. Wilusz, E. J. Wagner, K. Adelman, The Integrator Complex Attenuates Promoter-Proximal Transcription at Protein-Coding Genes. *Mol. Cell*. **76**, 738–752.e7 (2019).

65. D. C. Tatomer, N. D. Elrod, D. Liang, M.-S. Xiao, J. Z. Jiang, M. Jonathan, K.-L. Huang, E. J. Wagner, S. Cherry, J. E. Wilusz, The Integrator complex cleaves nascent mRNAs to attenuate transcription. *Genes Dev.* **33**, 1525–1538 (2019).

66. C. B. Stein, A. R. Field, C. A. Mimoso, C. Zhao, K.-L. Huang, E. J. Wagner, K. Adelman, Integrator endonuclease drives promoter-proximal termination at all RNA polymerase II-transcribed loci. *Mol. Cell*. **82**, 4232–4245.e11 (2022).

67. G. W. Muse, D. A. Gilchrist, S. Nechaev, R. Shah, J. S. Parker, S. F. Grissom, J. Zeitlinger, K. Adelman, RNA polymerase is poised for activation across the genome. *Nat. Genet.* **39**, 1507–1511 (2007).

68. M. Levine, Paused RNA polymerase II as a developmental checkpoint. *Cell*. **145**, 502–511 (2011).

69. K. Adelman, J. T. Lis, Promoter-proximal pausing of RNA polymerase II: emerging roles in metazoans. *Nat. Rev. Genet.* **13**, 720–731 (2012).

70. B. Gaertner, J. Zeitlinger, RNA polymerase II pausing during development. *Development*. **141**, 1179–1183 (2014).

71. R. Dollinger, D. S. Gilmour, Regulation of Promoter Proximal Pausing of RNA Polymerase II in Metazoans. *J. Mol. Biol*. **433**, 166897 (2021).

72. M. Noe Gonzalez, D. Blears, J. Q. Svejstrup, Causes and consequences of RNA polymerase II stalling during transcript elongation. *Nat. Rev. Mol. Cell Biol.* **22**, 3–21 (2021).

73. A. Abuhashem, V. Garg, A.-K. Hadjantonakis, RNA polymerase II pausing in development: orchestrating transcription. *Open Biol.* **12**, 210220 (2022).

74. J. B. Grimm, B. P. English, J. Chen, J. P. Slaughter, Z. Zhang, A. Revyakin, R. Patel, J. J. Macklin, D. Normanno, R. H. Singer, T. Lionnet, L. D. Lavis, *Nat. Methods*, in press.

75. Q. Zheng, A. X. Ayala, I. Chung, A. V. Weigel, A. Ranjan, N. Falco, J. B. Grimm, A. N.

Tkachuk, C. Wu, J. Lippincott-Schwartz, R. H. Singer, L. D. Lavis, Rational Design of Fluorogenic and Spontaneously Blinking Labels for Super-Resolution Imaging. *ACS Cent Sci*. **5**, 1602–1613 (2019).

76. Y. Chen, N. Kotian, J. A. McDonald, Quantitative Image Analysis of Dynamic Cell Behaviors During Border Cell Migration. *Methods Mol. Biol.* **2626**, 193–217 (2023).

77. T. U. Banisch, I. Maimon, T. Dadosh, L. Gilboa, Escort cells generate a dynamic compartment for germline stem cell differentiation via combined Stat and Erk signalling. *Development*. **144**, 1937–1947 (2017).

78. Y. Qiu, D. S. Gilmour, Identification of Regions in the Spt5 Subunit of DRB Sensitivity-inducing Factor (DSIF) That Are Involved in Promoter-proximal Pausing. *J. Biol. Chem.* **292**, 5555–5570 (2017).

79. E. D. Andrulis, E. Guzmán, P. Döring, J. Werner, J. T. Lis, High-resolution localization of Drosophila Spt5 and Spt6 at heat shock genes in vivo: roles in promoter proximal pausing and transcription elongation. *Genes Dev.* **14**, 2635–2649 (2000).

80. K. Hanyu-Nakamura, H. Sonobe-Nojima, A. Tanigawa, P. Lasko, A. Nakamura, Drosophila Pgc protein inhibits P-TEFb recruitment to chromatin in primordial germ cells. *Nature*. **451**, 730–733 (2008).

81. R. Fujiwara, S.-N. Zhai, D. Liang, M. Tracey, X.-K. Ma, A. P. Shah, C. J. Fields, M. S. Mendoza-Figueroa, M. C. Meline, D. C. Tatomer, L. Yang, J. E. Wilusz, IntS6 and the Integrator phosphatase module tune the efficiency of select premature transcription termination events. *bioRxiv* (2023), p. 2023.03.05.531184.

82. X. Long, J. Colonell, A. M. Wong, R. H. Singer, T. Lionnet, Quantitative mRNA imaging throughout the entire Drosophila brain. *Nat. Methods*. **14**, 703–706 (2017).

83. H. M. T. Choi, M. Schwarzkopf, M. E. Fornace, A. Acharya, G. Artavanis, J. Stegmaier, A. Cunha, N. A. Pierce, Third-generation in situ hybridization chain reaction: multiplexed, quantitative, sensitive, versatile, robust. *Development*. **145** (2018), doi:10.1242/dev.165753.

84. J. Schindelin, I. Arganda-Carreras, E. Frise, V. Kaynig, M. Longair, T. Pietzsch, S. Preibisch, C. Rueden, S. Saalfeld, B. Schmid, J.-Y. Tinevez, D. J. White, V. Hartenstein, K. Eliceiri, P. Tomancak, A. Cardona, Fiji: an open-source platform for biological-image analysis. *Nat. Methods*. **9**, 676–682 (2012).